

Influence of disorder on the vortex-lattice melting in twinned oxygen-deficient ortho-II $\text{YBa}_2\text{Cu}_3\text{O}_y$ ($y \approx 6.6$)

E. Rodríguez

Laboratorio de Bajas Temperaturas, Facultad de Ciencias Exactas y Naturales, Universidad Nacional de Buenos Aires, Ciudad Universitaria, Pabellón I, 1428 Buenos Aires, Argentina

and Institut de Ciència de Materials de Barcelona, Consejo Superior de Investigaciones Científicas, Campus de la Universitat Autònoma de Barcelona, 08193 Bellaterra, Spain

A. Gou, B. Martínez, S. Piñol, and X. Obradors

Institut de Ciència de Materials de Barcelona, Consejo Superior de Investigaciones Científicas, Campus de la Universitat Autònoma de Barcelona, 08193 Bellaterra, Spain

(Received 11 November 1997)

We investigated with ac susceptibility the mixed state of twinned, deoxygenated single crystals and highly c -axis-oriented melt-textured samples of $\text{YBa}_2\text{Cu}_3\text{O}_{6+x}$ with oxygen stoichiometry corresponding to that of the orthorhombic II phase. In the single crystal we found, below $H^* \approx 700$ Oe and over almost four orders of magnitude in frequency, a frequency-independent “irreversibility line” (IL). Complementary dc magnetization measurements seem to disregard an IL arising from geometric effects when $H \parallel c$, and they suggest a possible meltinglike transition of the flux-line lattice below H^* . The reduced value of H^* is associated with the increased anisotropy induced by the oxygen depletion, and an upper limit of the anisotropy parameter is estimated as $\gamma_{\text{max}} \approx 147$. However, in the twinned melt-textured sample having a major grade of disorder due to the presence of micrometric nonsuperconducting precipitates of Y_2BaCuO_5 , the IL is frequency dependent for all applied magnetic fields, suggesting a cancellation of H^* in the sufficiently disordered specimen. [S0163-1829(98)07613-9]

I. INTRODUCTION

After huge experimental and theoretical effort in the last years, it is now widely recognized that anisotropy and disorder are true keywords when interpreting the magnetic properties of high-temperature superconductors (HTSC's).¹ Properties of vortex pinning in HTSC's depend on the type and density of defects generating static disorder in the compounds and, moreover, a same class of defects can be expected to influence differently the irreversible behavior in materials with different anisotropy. On the other hand, vortex-lattice transformations as detected by means of transport measurements,² ac susceptibility,³ and magnetization,⁴ and interpreted as evidence of, e.g., melting or decoupling, have been found to be strongly dependent on both the anisotropy and the grade of disorder.^{5,6} However, despite the vast experimental work conducted to gain insight into the disorder-anisotropy interplay, not much attention has been focused on the study of the vortex structure in other high- T_c materials other than the moderate anisotropic $\text{YBa}_2\text{Cu}_3\text{O}_{6+x}$ (YBCO), with $6+x \approx 7$ and anisotropy parameter $\gamma = (M_{\perp}/M_{\parallel})^{1/2} \approx 5-7$,⁷ and the highly anisotropic $\text{Bi}_2\text{Sr}_2\text{CaCu}_2\text{O}_{8+\delta}$ (BSCCO), with $\gamma \approx 50-200$.⁷ Consequently, we have begun to investigate the characteristics of the phase diagram of deoxygenated samples of $\text{YBa}_2\text{Cu}_3\text{O}_{6+x}$ for which, as is well documented,⁸ the anisotropy can be finely tuned by controlling the oxygen content in the compound: So this system is potentially engaging in order to extend the studies mentioned above.

In the present work we will focus our interest on the so-

called orthorhombic II phase (O-II) of $\text{YBa}_2\text{Cu}_3\text{O}_{6+x}$, which with ideal oxygen stoichiometry $x = 0.5$ is responsible for the appearance of a second plateau in the $T_c(x)$, at oxygen contents of $0.45 < x < 0.65$ and transition temperatures about $T_c = 55-60$ K, besides the plateau existing close to $x \approx 1$ and $T_c = 90$ K.⁹ The ac susceptibility technique is used to show that in O-II YBCO a sharp transition in the vortex matter may manifest in single-crystalline samples at low magnetic fields $H \parallel c$. We found that the maximum field H^* up to which such a transition persists is strongly reduced with respect to that of fully oxygenated $\text{YBa}_2\text{Cu}_3\text{O}_7$ and it is argued that this is a consequence of the enhanced anisotropy induced by the oxygen content reduction. Also, we analyze the influence that defects with varied topology have on the possible transition in the vortex lattice. This is made by measuring and comparing the features of the irreversibility line in single-crystalline and melt-textured samples.

II. EXPERIMENT

A. Samples

The preparation of high-quality samples in the O-II phase is in the root of our experimental work. The samples studied were $\text{YBa}_2\text{Cu}_3\text{O}_{6+x}$ single crystals (SC's) grown, in gold crucibles, by a modified version of the self-flux method of Schneemeyer *et al.*,¹⁰ and highly oriented melt-textured (MT) $\text{YBa}_2\text{Cu}_3\text{O}_{6+x}:\text{Y}_2\text{BaCuO}_5$ (123:211) composites cleaved from “quasi-single-crystalline” pieces, processed by using a directional solidification technique based on the vertical Bridgman configuration.¹¹ The oxygen stoichiometry x

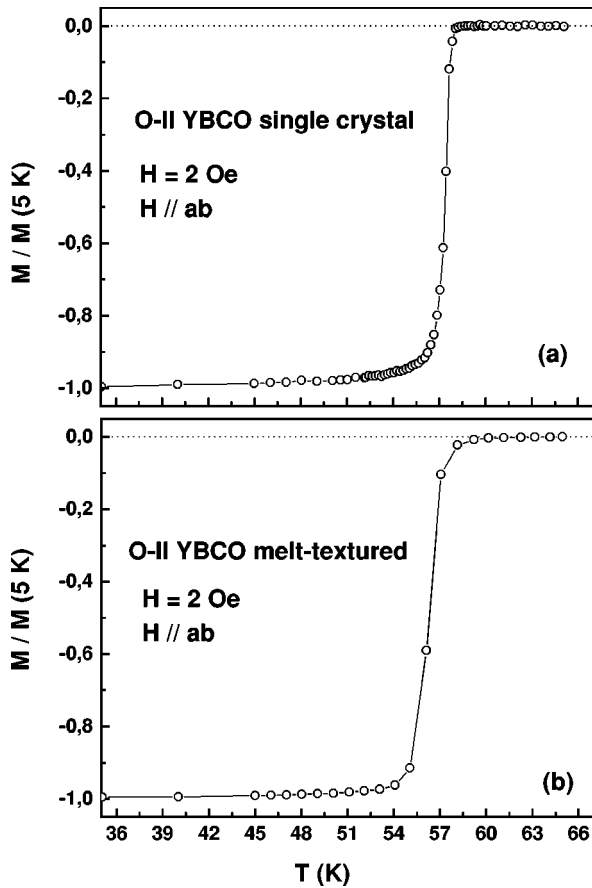


FIG. 1. Zero-field-cooling magnetization curves of (a) a single-crystalline and (b) a melt-textured ortho-II $\text{Yb}_2\text{Cu}_3\text{O}_{6+x}$ ($x \approx 0.6$) samples at $H = 2$ Oe perpendicular to the c axis.

corresponding to the O-II phase was adjusted by annealing the as-grown samples at about 600°C for 7 days in air and subsequently quenching them into liquid nitrogen. To assure we are dealing with samples on the second T_c versus x plateau of our YBCO system, and so with samples with an O-II superstructure, the suitable annealing temperature was determined from the study of the $T_c(x)$ curves for both the SC and the MT samples.¹² Long annealing times seem to be crucial to get a homogeneous oxygen distribution in the bulk, especially in the case of single crystals. From zero-field-cooled (ZFC) dc magnetization measurements in a low magnetic field (2 Oe), oriented perpendicular to the c -axis direction, the resulting superconducting transition temperatures T_c of the SC and the MT samples were determined to range between 56 and 59 K (Fig. 1) with transition widths [ΔT_c (10–90%) criterion] about 1 K for the single crystals and less than 3 K for the melt-textured crystals, typically double those found for the corresponding fully oxygenated state.

The oxygen stoichiometry x of the samples was about $x \sim 6.55$ – 6.60 as estimated by comparing the onset of the superconducting transition T_c with the previously published results for single-crystalline¹³ and ceramic¹⁴ samples.

Concerning the microstructure of the samples, the common defective background of both SC and MT samples is the high density of twin boundaries, as can be easily observed by polarized optical microscopy. However, MT samples also contain a relevant amount of micrometric inclusions of non-

superconducting Y_2BaCuO_5 (211), about 25% in weight, which are roughly homogeneously distributed in the 123 matrix.¹⁵ A small amount of CeO_2 (0.3 wt. %) is also present in these samples, intentionally added in order to refine the mean size of the 211 inclusions.¹⁶ The size distribution of the Y_2BaCuO_5 phase precipitates was deduced by means of an image analysis of scanning electron microscopy (SEM) pictures, from which the average diameter of the precipitates was determined to be $d < 1.4 \mu\text{m}$.¹⁷ In this work we will report on two samples, a single crystal and a melt-textured sample. The dimensions of these two samples were $1.30 \times 1.23 \times 0.22 \text{ mm}^3$ and $1.67 \times 1.31 \times 0.41 \text{ mm}^3$, respectively, with the shortest length along the c -axis direction. Their corresponding superconducting transition temperatures were $T_c = 57.8$ K and $T_c = 57.4$ K, as defined by the linear extrapolation of the magnetization to zero (see Fig. 1).

B. Measurements

The ac susceptibility experiments were performed in a miniaturized custom-made mutual inductance setup, consisting of a pair of carefully balanced secondary coils wound on a long primary coil. The ac excitation field h_{ac} was induced by an adjustable ac sinusoidal current flowing through the primary coil and obtained from the internal oscillator of a two-phase lock-in amplifier (EG&G 5210). The sample is glued to one of the secondary coils with its c axis perpendicular to the ac field. With this device we are able to measure the ac susceptibility response in a wide range of frequencies ($10 \text{ Hz} < f < 100 \text{ kHz}$) and alternating magnetic field amplitudes h_{ac} (from 250 mOe to several Oe). The susceptometer was incorporated in a ^4He gas flow cryostat where dc magnetic fields H_{dc} up to 55 kOe can be applied. The ac field was always perpendicular to the c axis of the samples, while the dc field was applied always parallel to the same axis ($h_{ac} \perp H_{dc} \parallel c$ configuration). In a typical run of the experiments the temperature was slowly swept ($dT/dt < 1 \text{ K/min}$) while both the in-phase (V') and the out-of-phase (V'') components of the complex voltage response, which are proportional to the change of the imaginary χ'' (dissipation) and real χ' (shielding) susceptibilities, respectively,¹⁸ were simultaneously monitored with the lock-in amplifier. All the ac susceptibility measurements have been taken in field-cooling conditions.

In addition to the ac measurements, dc magnetization measurements were carried out in a Quantum Design superconducting quantum interference device (SQUID) magnetometer with H along the c -axis direction. The thermal dependence of the critical current J_c^{ab} in a self-field of both kinds of samples (SC and MT) was determined inductively, from measurements of the remanent magnetization versus temperature, by using the generalized Bean model¹⁹ in which $J_c^{ab} = 40M_{irr}[a(1 - a/3b)]$, $a < b$ being the sample sides limiting the surface perpendicular to the applied field and M_{irr} the irreversible magnetization. Hysteresis loops $M(H)$ at different temperatures $t = T/T_c > 0.95$ were also recorded for the single crystal in the range $H < 800$ Oe.

III. RESULTS AND DISCUSSION

In ac susceptibility measurements the irreversibility line (IL) at a given dc field and fixed frequency of the ac field is

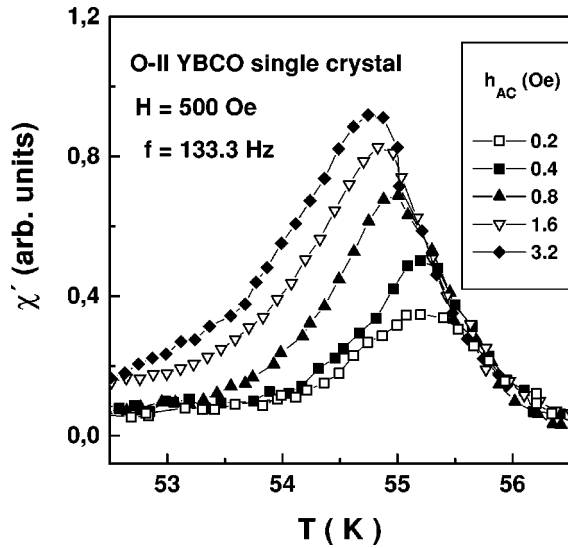


FIG. 2. Dissipation peaks χ'' as a function of temperature measured in the ortho-II single crystal at $f=133.3$ Hz in a dc field $H=500$ Oe parallel to the c axis for different amplitudes of the alternating excitation $h_{ac}\perp c$.

given by steering the criterion established by Civalé *et al.*:²⁰ By reducing the value of the amplitude of the excitation h_{ac} , the dissipation peak position $T_p(h_{ac})$ can be pushed to higher temperatures and it may be located at the onset of a nonlinear response, which is a suitable definition of the IL.²⁰ However, due to the limited sensitivity of our setup, together with the reduced sample dimensions, the above conditions are not completely satisfied down to the lower h_{ac} we can apply while preserving a good signal-to-noise figure. Figure 2 shows results of $\chi''(T)$ obtained in the O-II single crystal for several h_{ac} values at $f=133.3$ Hz with $H=500$ Oe. We note that, even though the low-temperature region of the dissipation peak and the position of its maximum T_p both vary with h_{ac} , T_p begins to saturate for values of h_{ac} below 0.4 Oe. On the contrary, the high temperature side of $\chi''(T)$ is seen to be h_{ac} independent within the experimental resolution, which in turn means that it lies in the region of linear response. So the maximum of $\chi''(T)$ at the lowest applied h_{ac} fields roughly separates regions of linear and nonlinear behavior for all dc fields. In consequence, we track down the IL at the χ'' peak position determined at the lowest applied h_{ac} , i.e., $h_{ac}=0.25$ Oe, and feel it is a reasonable definition of the experimental IL we shall present.

More relevant results have been obtained when measuring the frequency dependence of the IL for the SC, with the above-mentioned criterion concerning the h_{ac} parameter. Figure 3 shows the lines determined from the positions of the maxima of the dissipation peaks $\chi''(T)$ measured at $h_{ac}=0.25$ Oe for various frequencies of the ac excitation and in different dc magnetic fields. A striking feature is observed at low dc magnetic fields $H < H^* \approx 700$ Oe: The defined IL is almost frequency independent for about four orders of magnitude, within our temperature determination accuracy. This fact can be most clearly noticed in Fig. 4(a) where we represent the Arrhenius plots of the measuring frequency as a function of the inverse of the temperature at which the $\chi''(T)$ peak is detected, for different applied dc fields. The lines at $H < H^*$ show a change in frequency of four orders of mag-

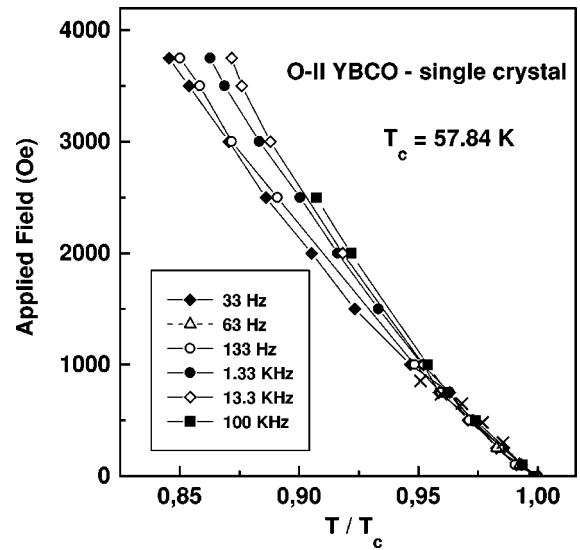


FIG. 3. Frequency dependence of the low-field "irreversibility line" of the single crystalline ortho-II $\text{Yba}_2\text{Cu}_3\text{O}_{6+x}$ specimen, with the frequency in the range $13 \text{ Hz} < f < 100 \text{ kHz}$. The symbols correspond to the maximum of the $\chi''(T)$ curves at $h_{ac}=0.25$ Oe ($h_{ac}\perp c$) for different applied dc fields ($H\parallel c$). The crosses correspond to the dc irreversibility line obtained from the hysteresis loops (see Fig. 6).

nitude within a temperature variation close to the experimental error in the determination of the temperature position of the dissipation peak, ± 0.05 K. On the other hand, for $H > H^*$ the IL is observed to shift towards lower temperatures when the excitation frequency is reduced (Fig. 3). This frequency dependence of the position of the dissipation peak appears as lines with a finite slope in the Arrhenius plots for $H > H^*$ [Fig. 4(a)].

Since measuring at a fixed frequency ac measurements in the linear regime explore a constant resistivity contour of the system,^{3,20} the observed low-field ($H < H^*$) frequency independence of the SC irreversibility line might be associated with a sharp drop in the temperature dependence of the resistance, therefore indicating that the vortex matter undergoes a drastic change at the irreversibility temperature $T_{irr}(H)$. A sharp "kink" in the resistivity is usually taken as the footprint of a melting phase transition in the vortex lattice of HTSC's.² Thus, although our ac susceptibility measurements do not unambiguously emulate the transport experiments, the appearance of a frequency-independent IL for $H < H^*$ strongly suggests the existence of a vortex melting phase transition within the system in the low-field and high-temperature region of the H - T diagram of the O-II phase single crystal. In fact, the sharp hysteretic drop observed in the linear response resistance of oxygen stoichiometric twin-boundary-free YBCO crystals has demonstrated the first-order character of the melting transition of the vortex lattice.² Also, a frequency-independent IL, reported for BSCCO single crystals up to 360 Oe, with a similar experimental configuration as ours concerning h_{ac} and H , has been interpreted as a manifestation of a first-order decoupling transition.³

In contrast, for $H > H^*$ the transition becomes continuous as follows from the fact that the irreversibility line depends on the time scale of the measurements. Since the IL at each

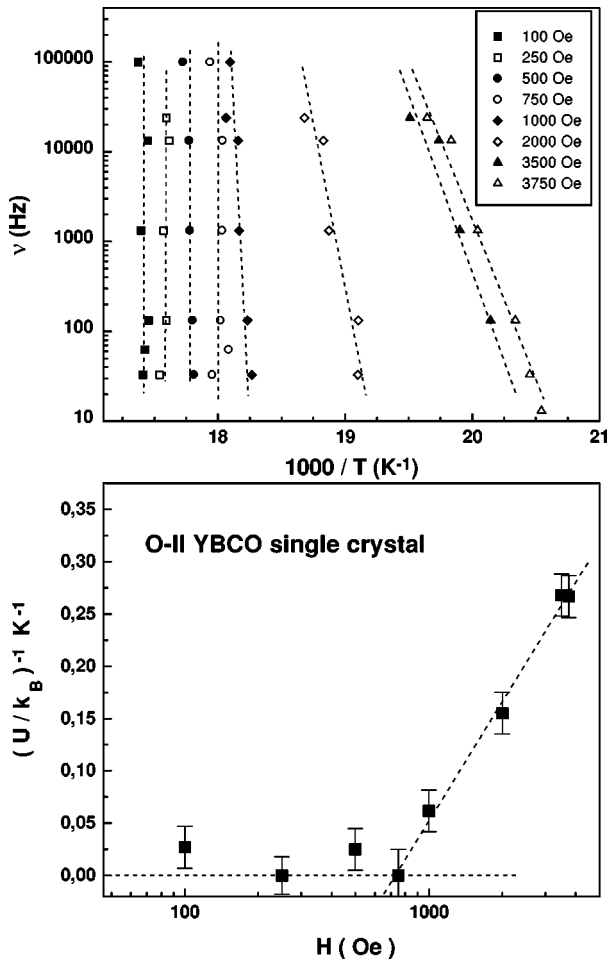


FIG. 4. (a) Arrhenius plots of the single crystal: the measuring frequency as a function of the inverse of the temperature corresponding to the peak of the dissipative component χ'' of the ac susceptibility, measured at $h_{ac}=0.25$ Oe for several applied dc fields. (b) Inverse of the activation energies obtained from the slopes of the Arrhenius plots, as a function of the applied field.

frequency can be assigned to a contour line of constant resistance, the frequency dependence of the IL implies smooth and continuous resistance vs temperature curves. That is, the resistance transitions for $H > H^*$ would present low-temperature smooth tails and broader widths than for $H < H^*$ where a sharp drop should be found. As can be deduced from the Arrhenius plots, a thermally activated process is the cause of the smooth temperature dependence of the resistivity at fields higher than H^* . The activation energies corresponding to that process can be obtained from the slope of the Arrhenius lines. Displayed in Fig. 4(b) are the inverses of the activation energies, $U^{-1}(H)$. It can be seen that the value of the energy barrier increases monotonically when decreasing the field down to H^* ; there a discontinuity appears and the activation energies start to diverge, thus indicating that the onset of the appearance of the sharp drop in resistivity is a phenomenon clearly not attributable to thermal activation. Broad resistive transitions, as opposite to the ones with the sharp drop, have been found for clean, untwinned YBCO single crystals above a certain field which it is seen to depend on the degree of disorder^{2,21} and also in twinned YBCO single crystals when $H \parallel c$ in all the

range of fields.²¹ Some of these transitions are demonstrated to be continuous second-order vortex-glass phase transitions. Besides this, in the already mentioned ac susceptibility measurements in BSCCO single crystals,³ the IL shows a frequency dependence down to 360 Oe, and so a continuous transition for $H > 360$ Oe.

It is very significant that the results of Fig. 3(a) strongly resemble the characteristics of the magnetic phase diagram of clean, untwinned, fully oxidized $\text{YBa}_2\text{Cu}_3\text{O}_7$ (Ref. 2) and clean BSCCO (Ref. 3) single crystals as well, and so it is tempting to conclude that the O-II phase SC preserves those characteristics of a clean system when presenting a sharp vortex-lattice transition in the low-field window of the phase diagram. However, as already mentioned, the SC used in our research contains a great number of twin boundaries (TB's). The presence of TB's in $\text{YBa}_2\text{Cu}_3\text{O}_7$ has already been recognized as inhibitory of the manifestation of the first-order phase transition in the vortex lattice when $H \parallel c$.²² This immediately raises questions about the role that the different types of defects play in this more anisotropic material. We discuss now the two effects that can explain why the TB's have a less remarkable effect in the phase diagram of the O-II system. First, the oxygen-deficient samples have a lower orthorhombicity factor than the nearly stoichiometric ones;^{13,14} this suggests the possibility that the reduction of the superconducting order parameter in the core of the TB's is smaller in the O-II phase, and hence the TB pinning strength is reduced. Second, and in agreement with the previous argument, the pinning of vortices in the c -axis-correlated TB's could convert itself in a less effective pinning process in the O-II phase, due to the higher anisotropy of this phase that leads to a quasi-two-dimensional behavior of the vortex lattice. In effect, transport experiments²³ performed on oxygen-deficient YBCO single crystals seem to support the idea of a weak effect of TB's on the vortex lattice in the O-II state and, for example, it has been found that the angular dependence of the magnetoresistance of deoxygenated and densely twinned 123 single crystals ($T_c = 56.9$ K) do not display evidence of vortex pinning by these planar defects in the $H \parallel c$ configuration.²³ In addition, torque magnetometry results also suggest that there is no specific contribution of the TB's to the pinning when $H \parallel c$ in aligned monocrystalline grains with reduced oxygen contents $x = 6.85$.²⁴ In both cases, it was said that the oxygen depletion makes the vortex system evolve towards a quasi-two-dimensional behavior, intrinsically linked to the increase of the anisotropy, for which the planar defects become ineffective in pinning. In that sense, recently, pseudo-flux-transformer (PFT) measurements have shown a continuous decrease of the c -axis vortex correlation in YBCO SC's when the oxygen content is lowered down to $x = 6.65$, in accordance with the enhancement in anisotropy yielded after the oxygen depletion.²⁵ This result clearly differentiates from the case found with identical PFT experiments in twinned, fully oxygenated single crystals, where a flux-line structure conforms the vortex state below and above the irreversibility temperature.²⁶ In the context of PFT results, the lower c -axis superconducting coupling results in a reduced vortex coherence between pancakes lying in adjacent layers, and reveals possible enhanced two-dimensional (2D) effects in the O-II system.²⁵

Further insight into the dimensionality of the vortex system can be obtained from our ac susceptibility experiments, thanks to the $h_{ac} \perp H$ configuration. The ac field applied parallel to the ab planes induces currents flowing across the Cu-O planes. In other words, the ac transversal field leads to a flux-line tilt that penetrates into the sample up to some diffusion length which depends on the tilt modulus of the elastic lattice, c_{44} , and on the Labusch parameter, i.e., on the pin restoring force. Therefore, we can conclude that when $h_{ac} \perp H$ our experiment is actually checking the coupling strength between the Cu-O planes and the vortex coherence along the c -axis direction. In fact, our experiment can detect the transition from a c -axis-coherent to a c -axis-incoherent state. In the coherence phase there is a finite effective penetration depth of the transversal ac field while in, e.g., an incoherent state of two-dimensional vortices, this depth diverges and the ac field is not screened at all. Taking all of this into account, we can now draw a picture of the vortex system properties in every region of the H - T phase diagram.

At $T < T_p$, the vortex lattice is supposed to be in a solid state, pinned by the different type of defects present in the material, and with a long-range superconducting order in all directions. When the ac probing weak field is applied perpendicular to this pinned vortex lattice, the flux lines start moving through the generation of kinks produced by short vortex segments, along the c -axis direction, jumping to new positions. This tilting process is the cause of the observed dissipation at $T < T_p$. As the degree of tilt grows with the h_{ac} amplitude, so will the dissipation, thus leading to the observed nonlinear behavior of the system (Fig. 2). As mentioned before, the c_{44} tilt modulus can also influence the appearance of dissipation in the sample. An infinite tilt modulus, due to a very rigidly pinned 3D vortex lattice, will not produce any dissipation. In contrast, weak pinning and large anisotropies make the vortex lattice softer, decreasing the c_{44} value and causing the appearance of dissipation, as seems to be the case for the O-II phase SC.

When $T > T_p$ the ac response of the system is linear, and so the skin depth model can be used to analyze the origin of the dissipation at the high-temperature side of the $\chi''(T)$ curves. Within this model, the maximum dissipation is known to occur when the diffusion length of flux (D) coincides with a characteristic dimension of the sample (l): $D = 5030/(\rho f)^{1/2} = l$, where D is in cm, f is in Hz, and ρ is the temperature-dependent resistivity in Ω cm. Considering our geometrical setup and the dimensions of the sample, it is easy to conclude that the skin depth condition will be first satisfied for the c -axis direction. This means that the high-temperature dissipation is due to the existence of a certain resistivity along the c -axis direction and not associated with currents flowing in the ab planes as would be the case if $h_{ac} \parallel H \parallel c$.

For $H < H^*$, it is significative that the frequency-independent ac IL coincides with the dc IL. This can be seen in Fig. 3(a) where the dc IL, defined as the field where the magnetization loop $M(H \parallel c)$ closes and the magnetization becomes reversible (see Fig. 6), is plotted together with the ac irreversibility lines. Considering that the dc IL has to be associated with currents flowing in the Cu-O planes, while our ac experiments, with $h_{ac} \perp c$, check currents crossing these planes, the coincidence of the two (dc and ac) irreversibility

lines implies that at this boundary the system crosses from a coherent state along all the directions of the sample to an incoherent or liquid state where the vortices can move freely, thus giving support to the idea that an independent frequency IL is the sign of a meltinglike phase transition of the vortex system. Since the dc SQUID measurements are equivalent to the ac ones with a characteristic frequency at least two orders of magnitude smaller than the minimum frequency used in the ac experiments, the close coincidence of the two IL's reinforces the frequency-independent behavior found for $H < H^*$.

For $H > H^*$, the existence of a nonzero c -axis resistivity can be related to a certain degree of decoupling of the Cu-O planes and so to a reduction of the phase coherence along the c axis. In that sense, the ac IL can be interpreted as a thermally activated decoupling line above which the vortex system acquires a more pronounced 2D character with a weaker phase coherence between planes and so a reduced length of the vortex line. So a quasi-2D vortex lattice is supposed to exist at $H > H^*$. At high temperatures, the melting of this quasi-2D vortex lattice is expected to be seen from measurements involving currents flowing in the ab planes. The observation of a dc IL lying below or above the ac IL line determined with $h_{ac} \parallel H$, depending on the frequency, would be a probe of a possible different origin of these ac and dc irreversibility lines above H^* . Attributing the first one to the decoupling of the pancakes lying within the Cu-O planes, the dc one could be related to the melting of the quasi-2D vortex lattice. This should be able to indicate if the O-II system loses its interplane coherence at a lower or higher temperature than it loses the in-plane coherence. Nevertheless the pseudo-flux-transformer results obtained at $H = 10$ kOe in deoxygenated YBCO (Ref. 25) seem to be consonant with the present picture when $H > H^*$. However, further ac susceptibility measurements, but with $h_{ac} \parallel H$, might also help to confirm the above speculated character of the vortex system for $H > H^*$, together with the origin of the dissipation origin in this range.

We now focus our attention on the field H^* below which the ac IL presents a frequency-independent behavior. First, it must be noted that through transport experiments in clean, fully oxidized $\text{YBa}_2\text{Cu}_3\text{O}_7$ ($T_c = 93$ K), Safar *et al.*² have shown that the field below which the sharp hysteretic resistivity transition is seen can be as high as 100 kOe, while for the O-II phase single crystal we purport a value as low as ~ 700 Oe. In the case that TB's do not play an important role in the present oxygen-deficient specimen, the strong reduction of H^* with respect to the corresponding value for the fully oxidized compound should be taken as a consequence of the enhancement in anisotropy after the oxygen depletion. It has been theoretically predicted by Glazman and Koshelev²⁷ that a 3D-2D crossover in the thermal fluctuation dimensional regime takes place in the layered superconducting compound at $B_{cr} \approx \phi_0 / (2\pi\gamma^2 s^2)$, where ϕ_0 is the flux quanta, γ is the anisotropy factor, and s is the interlayer spacing, occurring that for $B > B_{cr}$ the thermal fluctuations have a quasi-two-dimensional character as a consequence of the loss of the interlayer interaction. Assuming that our H^* is the crossover field described by Glazman and Koshelev, $B_{cr} = \mu_0 H^* \approx 700$ G, and taking $s = 11.7$ Å, we obtain for the O-II SC an anisotropy ratio of $\gamma = 147$, about a factor of 3

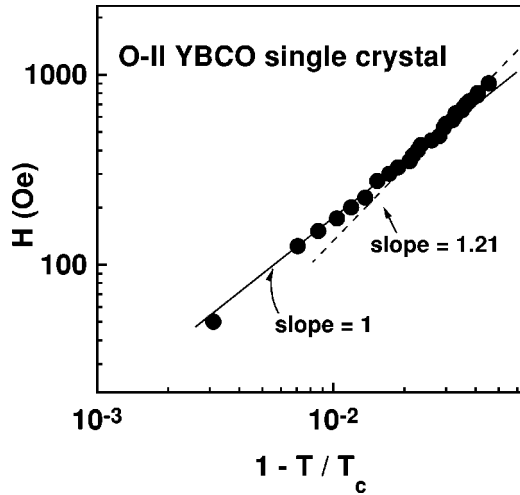


FIG. 5. Irreversibility line in the single crystal represented as H vs $(1 - T/T_c)$ on logarithmic scales, at $f = 133.3$ Hz. The lines are fits to a power law $H = H_0(1 - T/T_0)^\alpha$ with $\alpha = 1$ for $H < H^*$ (solid line) and with $\alpha = 1.21$ for $H > H^*$ (dashed line).

larger than the already published values.⁸ Glazmann and Koshelev²⁷ have not taken into account the effect of structural disorder in the possible phase transitions. However, it is well known that the strength of disorder can influence the nature of the transitions in the vortex matter.⁵ In our case, pointlike disorder (impurities in the matrix) or intrinsic lattice disorder avoiding long-range O-II order²⁸ is likely to contribute in anticipating B_{cr} .²⁹ Thus, our estimation of the anisotropy ratio γ may just be an upper limit for the value of this parameter in the single crystal. So H^* can be thought of as a disorder-dependent field beyond which the sharp transition gives way to a continuous one, due to the increase of the two-dimensional character of the system on increasing field and to the fact that the 2D systems are much more sensitive to disorder than the 3D ones. In this context H^* is not exactly the field where a 3D-2D fluctuation crossover takes place, as can be deduced from Ref. 27, but the field at which the system has acquired a certain 2D character so that a critical strength of disorder is attained, enough to suppress the sharp phase transition.

Further experimental information pointing to the different features of the vortex system below and above a crossing field can be found in Fig. 5, where a log-log plot of the IL of the SC at 133.3 Hz is shown. A clear change in the slope of the phase boundary is observed at a field close to H^* as determined from Fig. 3, where the transition goes from frequency independent to continuous: While IL's can be well described by a power law $H = H_0(1 - T/T_0)^\alpha$ in the whole range of applied magnetic fields, for $H < H^*$ the best fit to the data results in $\alpha = 1$, while $\alpha = 1.21$ if $H > H^*$.

Until now, all the results suggest to us the possibility that the low-field features of IL's in O=II YBCO single crystals could represent a meltinglike transition, similar to the first-order transition found in clean, fully oxygenated YBCO (Ref. 2) and clean BSCCO (Refs. 3 and 4) single crystals. To provide further independent support for the expected first-order character of the phase transition, a finite discontinuity in the magnetization has to be found.^{3,4} A frequency-independent IL, observed with a similar experimental con-

figuration concerning h_{ac} and H ,³ has already been reported in BSCCO. In Ref. 3 the feature was interpreted as a manifestation of a first-order decoupling transition, a notion which was reinforced by the observation of a jump in the thermodynamic magnetization (M_{rev}) at the irreversibility line. The value of the expected M_{rev} 's jump ΔM at the vortex melting transition for our system can be calculated using the Clausius-Clapeyron equation. According to this equation the change in entropy, in units of k_B , at the transition per vortex per Cu-O layer is given by

$$\Delta S = - \frac{s \phi_0}{k_B} \frac{\Delta M}{H_m} \frac{dH_m}{dT}, \quad (1)$$

where s is the interlayer distance and dH_m/dT is the slope of the melting line for $H < H^*$ (see Fig. 3). Taking for the melting transition the entropy change calculated by Monte Carlo simulations of Hetzel *et al.*,³¹ $\Delta S = 0.3k_B$ per vortex per layer, expression (1) yields a change in magnetization of $\Delta M = 1.5 \times 10^{-3}$ emu/cm³ at a field of about 270 Oe that can be deduced following the arguments presented in Ref. 31, and using the parameters of our system: $s = 11.8$ Å and $\gamma = 147$. The magnitude of the magnetization jump is very sensitive to the anisotropy; therefore we can obtain very different step values $8.7 \times 10^{-3} < \delta M$ (emu/cm³) $< 4.0 \times 10^{-2}$ when using the previously published anisotropy data, $\gamma = 20-50$,⁸ instead of our determined upper limit for this parameter. Nevertheless, due to the small dimensions of our single crystal, even for the best case (that is, assuming the lowest anisotropy) the magnitude of the expected step is near our present limit of resolution for detecting changes in magnetization as to withdraw its observation. Furthermore, demagnetization effects, when taken into account, could reduce the above calculated ΔM by a factor of $1/(1-n)$, which for a typical platelet geometry will be of order of 10–100, with n the demagnetization factor.³² On the other hand, it was also suggested that the observation of the ΔM jump may also be unnoticeable if global magnetization measurements are performed in a thin plateletlike crystal in the perpendicular geometry at low fields, due to the nonuniformity of the internal magnetic field.³² The inhomogeneous distribution of this field inside the crystal implies that the transition would take place at different values of temperature or applied field at different points of the sample, thus smoothing or even hiding the global magnetization jump.

A highly nonuniform internal field could be due to the presence of geometrical barriers.³² Then if geometrical effects were relevant in our system in the low-field, high-temperature region, the IL in this H - T regime could have its origin in the presence of these barriers, as already proposed for BSCCO below about $H < 200$ Oe and $T/T_c > 0.7$.³² Therefore the observed frequency independence of the IL can be thought of as a natural consequence of such mechanism, which is suggested to be quasiexempt of the effects of thermal activation.³² In order to check the possible existence of geometrical effects we have measured some magnetization hysteresis loops $M(H)$ at $T < T(H^*)$ and in a field regime crossing H^* . It was demonstrated that if the entrance and exit of vortices in the sample are mostly driven by geometrical barriers, the two branches of the loop should be asymmetric on ascending and descending fields. However, as

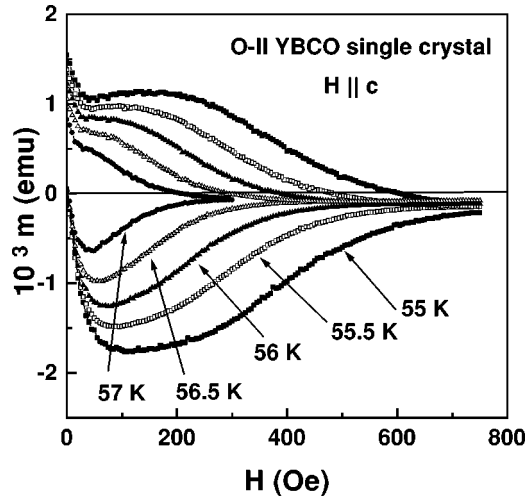


FIG. 6. Magnetic hysteresis loops of the ortho-II single crystal taken at several temperatures above $T(H^*)$. The field is applied along the c axis.

shown in Fig. 6, the magnetization curves $M(H)$ look like those usually found when hysteresis is due to bulk pinning, the only asymmetry being the one caused by the reversible magnetization. So these results, in principle, deny a purely geometrical origin of the magnetic irreversibility observed in $H^*(T)$.

Therefore, we can conclude that the observed frequency independence of the IL, close to the linear-to-nonlinear crossover in $\chi''(T)$ below H^* (Fig. 3), is due to a drastic change of the SC resistivity which could be related to a melting-like transition of the vortex lattice. The presence of a large amount of twin boundaries does not seem to affect the sharp character of this phase transition in the restricted field range $H < H^*$.

In order to consider the role of other disorder sources on the magnetic phase diagram of the O-II system we now turn to the results for the melt-textured sample. Figure 7 shows the critical current $J_c^{ab}(H||c)$ in a self-field for both the single-crystal and the melt-textured samples as a function of temperature. It can be clearly seen that the J_c^{ab} 's for the MT specimen are higher, in almost all of the studied temperature range, than those of the SC and, what is even more important, the thermal dependence of the J_c^{ab} 's is stronger in the latter. These results make evident that some fundamental difference exists between the flux pinning mechanisms in the single crystal and those in the melt-textured sample, which can be attributed to an active role of the 211 precipitates in the pinning process of flux lines: Although the mean size of these precipitates is much larger than the ab -plane coherence length, $d \gg \zeta_{ab}$, the 211 inclusions provide a vortex-pinning-site interaction through the sharp 211/123 interface (where the superconducting order parameter ζ changes drastically), thus becoming an effective short-range interfacial pinning source.³³

The degree and type of disorder are known to change the nature of the phase transitions in the H - T diagram. In highly disordered systems the vortex liquid is predicted to experiment a second-order phase transition into a vortex-glass state³⁴ or into a Bose-glass state,³⁵ while, in very clean systems a first-order transition to an Abrikosov vortex lattice is

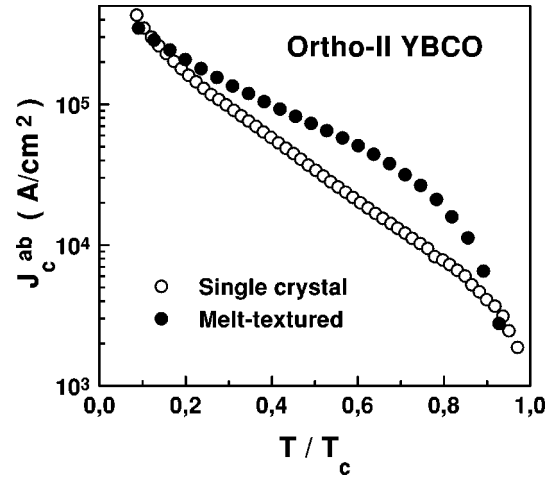


FIG. 7. Temperature dependence of the critical currents J_c^{ab} in a self-field (zero external applied field) deduced from remanent magnetization measurements for the single crystalline and the melt-textured samples. The samples were cooled under a magnetic field of 55 kOe from $T > T_c$ down to 5 K where the field was removed, and then the magnetization was measured as the temperature was slowly increased up to T_c . The inductive critical currents were determined by using the anisotropic Bean model.

thought to occur.^{30,36} Therefore, we expect that the added uncorrelated disorder in the O-II system, i.e., the 211 inclusions, will affect the sharp transition found in the SC at low fields in a similar manner as pointlike defects do when they are incorporated in fully oxygenated, clean $\text{YBa}_2\text{Cu}_3\text{O}_{6+x}$ single crystals through electron irradiation.⁵ It has to be remarked that the employment of MT specimens should not represent a handicap for the complement of the above experiments on SC's, since the MT samples are cleaved from a highly oriented single-domain piece, where the submosaic disarrangement ranges between 1° and 6° , as observed by careful x-ray analysis and transmission electron microscopy.³⁷

Figure 8 shows the frequency dependence of the IL for the melt-textured sample containing 25 wt. % of micrometric 211 precipitates. The comparison with the results of Fig. 3 is straightforward: The IL of the MT is found to be frequency dependent for all dc fields, a behavior that clearly differentiates from that in the SC, where there exist a nonzero dc magnetic field H^* below which the IL is frequency independent. This means that the MT sample undergoes a vortex-liquid-to-solid continuous transition, instead of a sharp one, in all the studied range of fields. The Arrhenius plots for the MT shown in Fig. 9 point to a thermally activated process as being responsible for the continuous vortex freezing in the H - T plane for the MT sample. So the comparison between the SC and the MT phase diagrams makes evident the cancellation of H^* in the melt-textured sample which has a similar T_c than the SC, but extra disorder due to the presence of the 211 inclusions. In that sense, this result resembles the previous finding on irradiated 123 untwinned single crystals in Ref. 5 where it is reported that the first-order vortex-liquid-to-solid phase transition found for the preirradiated crystal can be suppressed by the controlled introduction of point defects via electron irradiation. Thus, within a global context, our results fall into the general contention that dis-

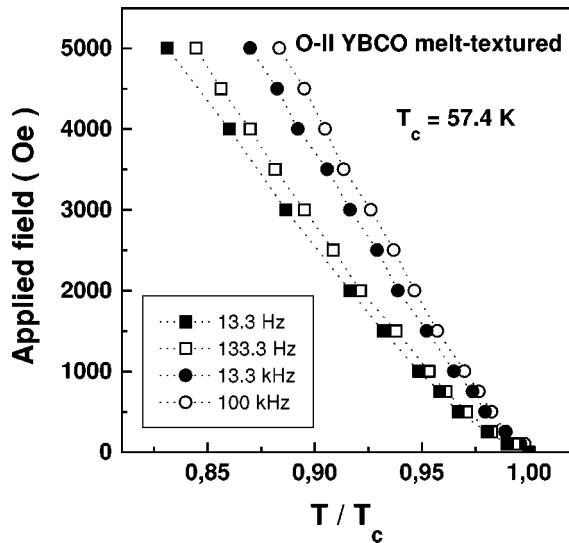


FIG. 8. Frequency dependence of the low-field $H < 5$ kOe, $H \parallel c$ "irreversibility line" of the melt-textured ortho-II specimen, at different frequencies ranging between 13 Hz and 100 kHz. The symbols correspond to the maximum of the $\chi''(T)$ curves at $h_{ac} = 0.25$ Oe with $h_{ac} \perp c$ for different applied dc fields $H \parallel c$.

order plays an important role in canceling possible first-order phase transitions in the vortex structure of high-temperature superconductors and tuning them into continuous ones. Moreover, our results provide further evidence that disorder becomes the determining parameter in controlling the different behavior in systems with similar anisotropy and they can be helpful on conforming the H - T anisotropy-disorder phase diagram.

IV. CONCLUSIONS

Concluding, ortho-II YBCO single-crystalline and melt-textured samples with similar oxygen content and similar T_c , likely showing the same anisotropy, strikingly differentiate their vortex behavior depending on the grade and class of disorder. A sharp transition, attributed to the flux lattice melting, has been identified in the single-crystalline O-II YBCO sample below a characteristic field H^* which is

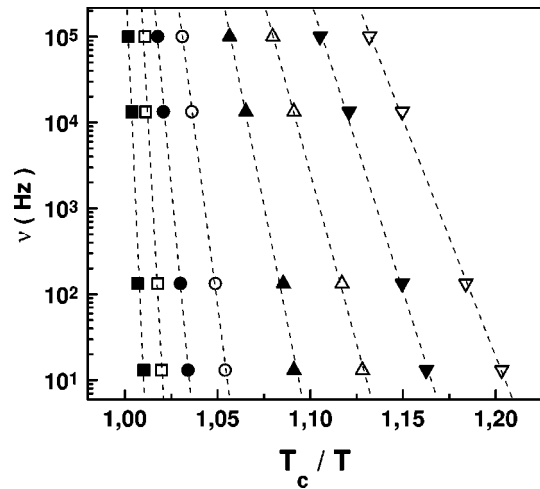


FIG. 9. Arrhenius plots of the ortho-II melt-textured sample: the measuring frequency as a function of the temperature at the χ'' peak for several applied dc fields. From left to right, data correspond to $H = 100, 250, 500, 1000, 2000, 3000, 4000,$ and 5000 Oe.

strongly reduced with respect to that in fully oxidized YBCO. The extra dense noncorrelated disorder provided by micrometric nonsuperconducting precipitates immersed in the 123 matrix of melt-textured samples seems to be responsible for the absence of a corresponding transition in this material. Comparative phase diagrams for deoxygenated single-crystalline and melt-textured samples have been presented. As a notion, the results of the features of the irreversibility line in each type of system show qualitatively the importance of different disorder sources in determining the characteristics of the vortex state in anisotropic high-temperature superconductors.

ACKNOWLEDGMENTS

We are indebted to V. Gomis for his technical advice on using the magnetometer. This work was financially supported by CICYT (MAT91-0742), Programa MIDAS (93-2331), and EC-EURAM (BRE2CT94-1011) projects. E.R. and A.G. would also like to thank the Ministerio de Educación y Ciencia of Spain for support.

- ¹G. Blatter, M. V. Feigel'man, V. B. Geshkenbein, A. I. Larkin, and V. M. Vinokur, *Rev. Mod. Phys.* **66**, 1125 (1994).
- ²H. Safar, P. L. Gammel, D. A. Huse, D. J. Bishop, J. P. Rice, and D. M. Ginsberg, *Phys. Rev. Lett.* **69**, 824 (1992); H. Safar, P. L. Gammel, D. A. Huse, D. J. Bishop, W. C. Lee, J. Giapintzakis, and D. M. Ginsberg, *ibid.* **70**, 3800 (1993); M. Charalambous, J. Chaussy, and P. Lejay, *Phys. Rev. B* **45**, 5091 (1992); W. K. Kwok *et al.*, *Phys. Rev. Lett.* **72**, 1088 (1994); W. K. Kwok *ibid.* **72**, 1092 (1994).
- ³H. Pastoriza, M. F. Goffmann, A. Arribére, and F. de la Cruz, *Phys. Rev. Lett.* **72**, 2951 (1994).
- ⁴E. Zeldov, D. Majer, M. Konczykowski, V. B. Geshkenbein, V. M. Vinokur, and H. Shtrikman, *Nature (London)* **375**, 373 (1995); R. Liang, D. A. Bonn, and W. N. Hardy, *Phys. Rev. Lett.* **76**, 835 (1996); U. Welp, J. A. Fendrich, W. K. Kwok, G.

W. Crabtree, and B. W. Veal, *ibid.* **76**, 4809 (1996).

- ⁵J. A. Fendrich, W. K. Kwok, J. Giapintzakis, C. J. van der Beek, V. M. Vinokur, S. Fleshler, U. Welp, H. K. Viswanathan, and G. W. Crabtree, *Phys. Rev. Lett.* **74**, 1210 (1995).
- ⁶G. Yang, P. Shang, S. D. Sutton, I. P. Jones, J. S. Abell, and C. E. Gough, *Phys. Rev. B* **48**, 4054 (1993).
- ⁷D. E. Farrell *et al.*, *Phys. Rev. Lett.* **64**, 1573 (1990); D. E. Farrell, S. Bonham, J. Foster, Y. C. Chang, P. Z. Jiang, K. G. Vandervoort, D. J. Lam, and V. G. Kogan, *ibid.* **63**, 782 (1989); J. C. Martínez, S. H. Brongersma, A. Koshelev, B. Ivlev, P. H. Kes, R. P. Griessen, D. G. de Groot, Z. Tarnavski, and A. A. Menovsky, *ibid.* **69**, 2276 (1992).
- ⁸B. Janossy, D. Prost, S. Pekker, and L. Fruchter, *Physica C* **181**, 51 (1991); T. R. Chien, W. R. Datars, B. W. Veal, A. P. Paulikas, P. Kostic, Chun Gu, and Y. Jiang, *ibid.* **229**, 273 (1994).

- ⁹R. J. Cava, B. Batlogg, C. H. Chen, E. A. Reitman, S. M. Zahurak, and D. J. Werder, *Nature (London)* **329**, 423 (1987); *Phys. Rev. B* **36**, 5719 (1987).
- ¹⁰S. L. F. Schneemeyer, J. V. Waszczak, T. Siegrist, R. B. van Dover, L. W. Rupp, B. Batlogg, R. J. Cava, and D. W. Murphy, *Nature (London)* **328**, 601 (1987); D. L. Kaiser, F. Holtzberg, B. A. Scott, and T. R. McGuire, *Appl. Phys. Lett.* **51**, 1040 (1987).
- ¹¹S. Piñol, V. Gomis, B. Martínez, A. Labarta, J. Fontcuberta, and X. Obradors, *J. Alloys Compd.* **195**, 11 (1993).
- ¹²A. Gou (unpublished).
- ¹³B. W. Veal, A. P. Paulikas, H. You, H. Shi, Y. Fang, and J. W. Downey, *Phys. Rev. B* **42**, 6305 (1990).
- ¹⁴R. J. Cava, A. W. Hewat, E. A. Hewat, B. Batlogg, M. Mareziro, K. M. Rabe, J. J. Krajewski, W. F. Peck Jr., and L. W. Rupp Jr., *Physica C* **165**, 419 (1990).
- ¹⁵F. Sandiumenge, S. Piñol, X. Obradors, E. Snoeck, and C. Roucau, *Phys. Rev. B* **50**, 7032 (1994).
- ¹⁶S. Piñol, F. Sandiumenge, B. Martínez, V. Gomis, J. Fontcuberta, and X. Obradors, *Appl. Phys. Lett.* **65**, 1448 (1994).
- ¹⁷N. Vilalta, F. Sandiumenge, S. Piñol, and X. Obradors, *J. Mater. Res.* **12**, 38 (1997).
- ¹⁸See, for example, J. R. Clem, in *Magnetic Susceptibility of Superconductors and Other Spin Systems*, edited by R. A. Hein, T. L. Francavilla, and D. H. Liebenberg (Plenum Press, New York, 1992).
- ¹⁹E. M. Gyorgy, R. B. van Dover, K. A. Jackson, L. F. Schneemeyer, and J. V. Waszczak, *Appl. Phys. Lett.* **55**, 283 (1989); S. M. Sauerzopf, H. P. Wiesinger, and H. W. Weber, *Cryogenics* **30**, 650 (1990).
- ²⁰L. Civale, T. K. Worthington, L. Krusin-Elbaum, and F. Holtzberg, in *Magnetic Susceptibility of Superconductors and Other Spin Systems*, edited by R. A. Hein, T. L. Francavilla, and D. H. Liebenberg (Plenum Press, New York, 1992); L. Krusin-Elbaum, L. Civale, F. Holtzberg, A. P. Malozemoff, and C. Feild, *Phys. Rev. Lett.* **67**, 3156 (1991); L. Krusin-Elbaum, L. Civale, G. Blatter, A. D. Marwick, F. Holtzberg, and C. Feild, *ibid.* **72**, 1914 (1994).
- ²¹W. K. Kwok, S. Fleshler, U. Welp, V. M. Vinokur, J. Downey, G. W. Crabtree, and M. M. Miller, *Phys. Rev. Lett.* **69**, 3370 (1992).
- ²²S. Fleshler, W. K. Kwok, U. Welp, V. M. Vinokur, M. K. Smith, J. Downey, and G. W. Crabtree, *Phys. Rev. B* **47**, 14 448 (1993); D. López, E. F. Righi, G. Nieva, and F. de la Cruz, *Phys. Rev. Lett.* **76**, 4034 (1996).
- ²³S. Fleshler, W. K. Kwok, U. Welp, J. Downey, and G. W. Crabtree, *IEEE Trans. Appl. Supercond.* **3**, 1483 (1993).
- ²⁴B. Janossy, H. Gu, R. Cabanel, and L. Fruchter, *Physica C* **193**, 344 (1992).
- ²⁵E. F. Righi, D. López, E. A. Jagla, E. Osquiguil, G. Nieva, E. Morré, F. de la Cruz, and C. A. Balseiro, *Physica C* **260**, 211 (1996).
- ²⁶D. López, E. Rodríguez, G. Nieva, F. de la Cruz, and S. W. Cheong, *Physica B* **194-196**, 1977 (1994); H. Safar, P. L. Gammel, D. A. Huse, S. N. Majumdar, L. F. Schneemeyer, D. J. Bishop, D. López, G. Nieva, and F. de la Cruz, *Phys. Rev. Lett.* **72**, 1272 (1994).
- ²⁷L. I. Glazman and A. E. Koshelev, *Phys. Rev. B* **43**, 2835 (1991).
- ²⁸P. Schleger, R. A. Hadfield, H. Casalta, N. H. Andersen, H. F. Poulsen, M. von Zimmermann, J. R. Schneider, R. Liang, P. Dosanjh, and W. N. Hardy, *Phys. Rev. Lett.* **74**, 1446 (1995).
- ²⁹D. R. Nelson and V. M. Vinokur, *Phys. Rev. B* **48**, 13 060 (1993).
- ³⁰A. Houghton, R. A. Pelcovits, and A. Sudbo, *Phys. Rev. B* **40**, 6763 (1989); G. Blatter and B. I. Ivlev, *ibid.* **50**, 10 272 (1994).
- ³¹R. E. Hetzel, A. Sudbø, and D. A. Huse, *Phys. Rev. Lett.* **69**, 518 (1992).
- ³²E. Zeldov, A. I. Larkin, V. B. Geshkenbein, M. Konczykowski, D. Majer, B. Khaykovich, V. M. Vinokur, and H. Shtrikman, *Phys. Rev. Lett.* **73**, 1428 (1994); E. Zeldov *et al.*, *Europhys. Lett.* **30**, 367 (1995); see also R. A. Doyle, D. Liney, W. S. Seow, A. M. Campbell, and K. Kadowaki, *Phys. Rev. Lett.* **75**, 4520 (1995).
- ³³B. Martínez, X. Obradors, A. Gou, V. Gomis, S. Piñol, J. Fontcuberta, and H. Van Tol, *Phys. Rev. B* **53**, 2797 (1996).
- ³⁴D. S. Fisher, M. P. A. Fisher, and D. A. Huse, *Phys. Rev. B* **43**, 130 (1991).
- ³⁵D. R. Nelson and V. M. Vinokur, *Phys. Rev. Lett.* **68**, 2398 (1992).
- ³⁶P. L. Gammel *et al.*, *Phys. Rev. Lett.* **61**, 1666 (1988); D. R. Nelson and H. S. Seung, *Phys. Rev. B* **39**, 9153 (1989); D. R. Nelson, *Phys. Rev. Lett.* **60**, 1973 (1988).
- ³⁷F. Sandiumenge, N. Vilalta, X. Obradors, S. Piñol, J. Bassas, and Y. Maniette, *J. Appl. Phys.* **79**, 8847 (1996).